Elsevier Editorial System(tm) for Applied Catalysis B: Environmental

Manuscript Draft

Manuscript Number: APCATB-D-16-00119R1

Title: Cooperative action of Brønsted and Lewis acid sites of niobium phosphate catalysts for cellobiose conversion in water

Article Type: Research Paper

Keywords: Niobium phosphate;
Solid catalyst effective acidity;
Cellobiose hydrolysis;
Glucose dehydration;
5-hydroxymethylfurfural(HMF)

Corresponding Author: Prof. Antonella Gervasini, PhD

Corresponding Author's Institution:

First Author: Antonella Gervasini, PhD

Order of Authors: Antonella Gervasini, PhD; Paolo Carniti, Professor; Filippo Bossola, Dipartimento di Scienza e Alta Tecnologia, Univers; Vladimiro Dal Santo, Dr, PhD

DOI: 10.1016/j.apcatb.2016.04.012

ABSTRACT:

The lively acidic properties in water of niobium phosphate (NBP) catalyst and NBP modified samples by acidic treatments in HCl solutions at 0.1, 1.0, and 10 M concentration (NBP01, NBP1, and NBP10, respectively) have been exploited for the direct conversion reaction of cellobiose to hydroxymethylfurfural (HMF) at temperature of 80-130°C. Acidity of the samples was determined by liquid-solid titrations working in a modified HPLC line with basic solutions of phenylethylamine (PEA), used as base probe. As solvents, an apolar-aprotic one, cyclohexane, was used for determining the *intrinsic* acidity and water for the *effective* acidity. In addition, pyridine/water co-adsorption FT-IR experiments complemented the acidity study, and the results obtained confirmed the presence of both *water-tolerant* Lewis acid sites (LAS) and some residual Brønsted acid sites (BAS) on all the NBP samples. On NBP, the LAS to BAS ratio was 1.69, measured in cyclohexane, and only slightly decreased to 1.30, when measured in water. Catalytic activity was studied in a liquid-solid reaction line with fixed bed flow reactor working in complete recirculation. The reaction of HMF formation from cellobiose consists of three distinct catalytic actions: hydrolysis of the β-1,4-glycosidic bonds of cellobiose, isomerization of the formed glucose monomers to fructose, and cyclo-dehydration of fructose to HMF. Comparative catalytic results obtained with a sulfonic acid resin (Amberlite IR 120) showed that it was not able to form any HMF from cellobiose in the range of temperature studied, only cellobiose hydrolysis to glucose can be successfully achieved on the protonic acid resin.

Keywords:
Niobium phosphate,
Solid catalyst effective acidity
Cellobiose hydrolysis,
Glucose dehydration,
5-hydroxymethylfurfural (HMF).

1. Introduction

Niobium is an interesting catalytic species with acidic and redox properties, which has been used in several selective oxidation and acid-demanding reactions [1-3].

Niobium phosphate ($NbOPO_4$ hereafter called NBP) has a texture, acidic and catalytic properties similar to the most popular niobium oxide catalyst, but it has the advantage that it conserves these properties at higher temperatures [1,4]. Okazaki et al. [5,6] showed that amorphous niobium phosphate does not crystallize prior to 800°C and exhibits high catalytic activity even after heat treatment at temperatures as high as 500°C. Thanks to these features, it can promote some interesting acid-catalyzed reactions, such as 3,3-dimethyl-1-butene isomerization [7] and, in particular, reactions where water is concerned as reactant, solvent, or product, such as fructose dehydration to 5-hydroxymethyl-2-furaldehyde (HMF) and other reactions of biomass conversion [8-12].

One of the distinguishing feature of these materials is the resistance to water of the isolated Nb Lewis acid sites present at the surface, which can maintain lively catalytic activity in polar and protic solvents [4, 13], differently from many conventional LAS containing catalysts. Recently [13], it has been confirmed that the presence of *water-tolerant* acidic sites in hydrated niobic acid ($Nb_2O_5 \cdot nH_2O$) originates from the presence of the NbO_4-H_2O adducts, still having a residual positive charge and thus acting as LAS.

NBP is a higher protonic solid than the most well-known niobic acid catalyst [10,14]. Acetonitrile FT-IR experiments revealed that NBP shows the presence of medium strong Brønsted acid sites and medium strong LAS at the surface. Lewis acidity can be assigned to unsaturated Nb(V) sites, while, Brønsted acidity is mainly originated by POH groups, and in lesser extent by NbOH sites [14]. Notably, a similar behavior was reported also for TiO_4 tetrahedra dispersed on mesoporous silica [15] and for anatase [16], the latter showing an even higher density of *water-tolerant* LAS than niobic acid.

The *effective* acidity in water of niobic acid and NBP, together with other derived catalysts containing Nb, was experimentally demonstrated by various catalytic and characterization measurements, and it has been exploited for biomass valorization reactions taking place in water [9-12,17,18]. In general, these catalysts are active and selective in reactions of hydrolysis, isomerization and dehydration of the saccharidic biomass. Unfortunately, during these transformations, they suffer from serious deactivation due to the formation of the so called *humins* [19], which are insoluble in water and deposit on the catalyst surface causing loss of active surface and catalyst deactivation [12,18,20].

Saccharidic biomass, also obtained from waste agricultural and forestall residues, can be converted into interesting platform molecules such as HMF, from hexose polymers, or furfural, from pentose polymers [21-27]. For example, HMF possesses a high potential industrial demand; many versatile chemical intermediates can be generated from HMF by large scale transformations, such as 5-hydroxymethylfuranoic acid, 2-5-furandicarboxylic acid, 2,5-bis(hydroxymethyl)furan, and 2,5-furandicarboxaldehyde, among other compounds [28-30]. These compounds can be used as six-carbon monomers that could replace other petrochemical-based monomers. For example, 2,5-furandicarboxylic acid is able to replace terephthalic, isophthalic, and adipic acids in the manufacture of polyamides, polyesters, and polyurethanes [31,32].

This study provides evidences that NBP and modified materials obtained from it by acidic treatments can be successfully used as catalysts for the synthesis of HMF from cellobiose (Scheme S1 – Supporting Data), chosen as model molecule of the cellulose polymer. Cellobiose molecule is constituted by glucose units linked by β,1-4-glycosidic bonds. Cellobiose is much more difficult to hydrolyze than other disaccharides (sucrose and maltose, for example) because of the strong β,1-4 glycosidic bonds [33]. The peculiar characteristics of the acidic catalysts used in this work have permitted to realize the conversion of cellobiose to HMF in water under mild conditions of temperature.

The sample acidity has been characterized by liquid-solid titrations carried out in a modified liquid-chromatograph (HPLC) by basic solutions of phenylethylamine (PEA) in different solvents. The *intrinsic* acidity was determined in cyclohexane, an apolar-aprotic solvent that does not interact with the surface, while the *effective* acidity in water. The nature and concentration of the acid sites was further investigated by spectroscopic analysis also in the presence of water, mimicking the reaction environment.

2. Experimental section

2.1. Materials

NBP was kindly supplied from Companhia Brasileira de Metalurgia e Mineração (CBMM). It contains 66.7 wt.% of Nb_2O_5, 15.9 wt.% of P_2O_5, 2.1 wt.% of K_2O, and 15.3 wt.% of H_2O.

Other samples obtained by acidic treatments of NBP in HCl at 0.1 M, 1.0 M, and 10 M concentrations (NBP01, NBP1, and NBP10, respectively) have been made. For the preparation of the NBP01, NBP1, and NBP10 samples, weighted amounts of dried NBP (at 120°C for a night) were soaked in 25 mL of HCl at fixed concentration (0.1, 1.0, and 10 M) and maintained under vigorous stirring for 1 h at room temperature. Then, the samples were filtered and thoroughly washed adding 25 mL of fresh water and maintaining the obtained suspensions under vigorous stirring for 1 h; the rinsing operation was repeated at least three times, up to neutrality of the collected waters. The samples were then dried at 120°C overnight. The NBP samples obtained from HCl treatment did not contain any chloride species derived from the preparation procedure, as revealed from EDX analysis (TM-1000 Tabletop Microscope, Hitachi Science Systems Ltd).

In the different experiments, NBP, NBP01, NBP1, and NBP10 have been used as powders and as particles of defined size after tableting; the powder samples were pressed and sieved as 20-40 mesh for the catalytic tests; 45-60 mesh for the morphologic analyses; 80-200 mesh for the acidity titrations.

2-Phenylethylamine (PEA), pyridine (Py), hydrochloric acid (37%) were purchased from Sigma- Aldrich. Cyclohexane and water (VWR, HPLC grade), were used for the liquid-solid acid titrations.

D-(+)-cellobiose (≥ 99%, Fluka), glucose (RPE, Carlo Erba), D-(+)-maltose (≥ 98%, Sigma-Aldrich), and D-(-) fructose (> 99%, Sigma) were used as substrate and standards for the various analyses.

The acidic resin (Amberlite IR-120 (H), Carlo Erba, referred as A120) is a styrene-divinylbenzene copolymer with sulfonic acid ($-SO_3H$) groups. A120 (a gel type resin) was supplied in the acidic form; before use it was rinsed with distilled water under stirring to remove mineral acidic residue, repeating the procedure until complete absence of color and acidity in the wash water. It was employed as particles of 0.3-1.1 mm size. The acid characteristics of A120 have been previously studied; it carries 2.27 mequiv/g of acidic centers, as measured in water by PEA titration [34].

2.2 Catalyst Characterization

Sample specific surface area ($m^2\ g^{-1}$), specific pore volume ($cm^3\ g^{-1}$), and pore size distribution were determined from N_2 adsorption and desorption isotherms measured at liquid nitrogen temperature with an automatic surface area analyzer (Sorptomatic 1900 instrument), the BET and BJH methods were employed for the computations. Prior to the measurement, the sample (ca. 100-150 mg), crushed and sieved as 45-60 mesh particles, was thermally activated at 120°C for 2 h under vacuum. The pore volume was determined from the total amount of N_2 adsorbed at P/P_0 = 0.99 using the N_2 density in the normal liquid state (ρ = 0.8081 g cm^{-3}). N_2 molecular area was taken as 16.2 $Å^2$.

The acidity measurements of the samples in liquid by using solutions of 2-phenylethylamine (PEA), as basic probe, were carried out in cyclohexane for the *intrinsic* acidity (I.A.) and in water for the *effective* acidity (E.A.). A recirculation chromatographic line (HPLC), comprising a pump (Waters 515) and a monochromatic UV detector (Waters, model 2487, λ = 254 nm) was used. The

sample (ca. 0.1 g crushed and sieved as 80-200 mesh particles) was placed in a sample holder (stainless steel tube, 2 mm i.d. and 12 cm of length), between two sand pillows. Prior to the measurement, the sample was activated at 150°C for 3 h in flowing air (8 mL min^{-1}) and then filled with the liquid (cyclohexane or water). The sample holder was mounted in place of the chromatographic HPLC column and maintained at constant temperature (30.0 ± 0.1°C). Successive dosed amounts of PEA (50 μL, *ca.* 0.10 M) were injected into the line in which the solution continuously circulated, until adsorption equilibrium was achieved. After the collection of the first adsorption isotherm of PEA on the fresh sample (I run), pure solvent was allowed to flow through the PEA-saturated sample up to the zero signal of the UV detector (this operation lasted between 40 and 60 min). Then, a new adsorption of PEA on the same sample was repeated (II run).

The collected isotherms have been interpreted following the Langmuir model (Equation 1):

$$PEA_{ads} / PEA_{ads,max} = b_{ads} [PEA]_{eq} /(1+ b_{ads} [PEA]_{eq} \quad (1)$$

From the conventional linearized equation, reporting $[PEA]_{eq}/PEA_{ads}$ *vs.* $[PEA]_{eq}$, the values of $PEA_{ads,max}$ (meq g^{-1}) could be obtained. Assuming a 1:1 stoichiometry for the PEA adsorption on the acid site, the value of $PEA_{ads,max}$ of the I run isotherm corresponded to the number of total acidic sites PEA_{tot}, while, the value of $PEA_{ads,max}$ (meq g^{-1}) obtained from the II run isotherm corresponded to the number of weak acidic sites, PEA_{weak}. The number of strong acid sites PEA_{strong} (meq g^{-1}) was obtained as the difference between the number of total and of weak sites.

Previous tests of PEA adsorption showed that it was adsorbed in negligible amount on samples without any acid and basic sites (sand, Fluka).

Lewis and Brønsted acid sites as well as their tolerance to water, were investigated by Fourier Transform Infrared Spectroscopy (FT-IR) (Biorad FTS-60A) using pyridine as probe molecule both in vapor phase and aqueous solution [35]. All the samples were pressed into 10-15 mg self-supporting disks (0.65 cm^2 geometrical area) and before each analysis they were calcined for 2 h at 150 °C in air. After outgassing for 30 minutes in high vacuum the samples were contacted with pyridine vapors at room temperature for 10 minutes or, alternatively, a $1x10^{-3}$ M pyridine aqueous

solution was dropped on self-supporting disks under argon flow. After pyridine adsorption, the samples were outgassed for 30 minutes in high vacuum at different temperatures (i.e. RT, 50, 100, 150, 200, 250°C). BAS and LAS concentrations, expressed as milliequivalents of adsorbed pyridine per gram of catalyst ($meq_{Py}\ g_{cat}^{-1}$), were determined by integrating the peaks at 1540 and 1448 cm^{-1}, respectively, of the spectra collected after outgassing at 150°C, according to the procedure reported by Emeis [36].

Thermogravimetric experiments (TGA7, from Perkin Elmer) were realized on the used catalysts after the catalytic tests to evaluate the amount of carbon-residues deposited on the catalyst surfaces [37]. Prior to the analysis, the sample discharged from the reactor was dried at 80°C for 2 h; then, an amount of 10-20 mg was put on the pan of the TGA and the temperature was allowed to increase from 50° to 800°C at 10°C min^{-1} under air flowing. The data were stored and processed by the Pyris Software.

2.3 Catalytic Activity

The tests of catalytic conversion of cellobiose were performed in liquid water in a total recirculation reaction line schematically shown in Fig. 1. The line can work up to 10 bar pressure in order to keep the fed solution in the liquid phase. The apparatus comprises: a liquid-chromatographic pump (Merck-Hitachi, L-6200 Intelligent Pump), a stainless steel pre-heater and fixed-bed flow reactor (172 mm long, 4.7 mm internal diameter and 6.4 mm external diameter) thermostated at the reaction temperature and put into a thermostatted oven, and a jacketed reservoir maintained at 17°C by cold water circulation, in which was put the feeding solution (typically 50 mL) and that received the reaction mixture coming from the reactor, that continuously recirculated; the total volume of the circulating solution was 78 mL. At the exit from the reactor, a cooling system with a coil immersed in cold water (17°C) allowed the solution to cool down. After the cooling system, a double micrometric valve allowed to regulate and maintain the pressure in the line.

The catalyst sample (ca. 1 ml, 20-40 mesh particles) was held in the middle of the reactor, between two sand pillows. The initial cellobiose aqueous solution (50 mM concentration) continuously circulated (3 mL min^{-1}) through the reaction line and on the solid catalyst maintained at constant temperature in a range 80°-130°C up to 100 h. Through this operative procedure, kinetic study could be realized by withdrawals of given amount of solution (ca. 0.1 ml) from the reservoir, and the catalyst stability could be investigated as well.

The reaction products (20 μL) were analyzed by a liquid chromatograph (HPLC) with an injector (Waters U6K), a pump (Waters 510), an oven for the thermoregulation of the column (Waters, model CHM), a refractive index detector (Waters 410) operating at 40°C, and a Hewlett Packard interface (model 35900). For qualitative and quantitative analyses, two columns were employed: a Sugar-Pak-I (Waters), operating at 90°C and eluted with a solution of Ca-EDTA 10^{-4} M in water (0.5 mL min^{-1}), and a Carbohydrate Analysis (Waters), suitable for volatile compounds and organic acids, operating at room temperature and eluted with acetonitrile/water 80:20 (0.5 mL min^{-1}). Calibrations have been carried out with standard solutions of cellobiose, glucose, fructose, HMF, furfural, levulinic and formic acids at different concentrations in the range of concentrations used in the activity tests.

In all the catalytic tests, the unreacted cellobiose and the formed reaction products (glucose, fructose, HMF, and a soluble condensation product not yet identified and indicated as CP1) have been quantified and expressed in terms of mono-saccharides equivalents. It was not possible to quantify a small amount of other soluble by-products formed, that corresponded on average to less than 5%.

The comparison between the total chromatographic areas of the soluble products and of cellobiose analyzed during the reaction with the initial area of cellobiose allowed to quantify the formation of insoluble products.

2.4. Kinetic Interpretation

The hydrolysis of cellobiose in water excess can be considered as a *pseudo*-first order reaction and when the reactor works as an ideal plug flow reactor, the following kinetic equation holds:

$$C_F = C_R \cdot \exp(-k\theta) \quad (2)$$

$$\theta = v/u \quad (3)$$

where C_R and C_F are the inlet and outlet concentrations of cellobiose into and from the catalytic bed, respectively, k the rate coefficient, θ the contact time, v the volume of the catalytic bed and u the flow rate.

When the flow rate is sufficiently high and the reaction rate is sufficiently low, the influent (C_R) and effluent (C_F) substrate concentrations to and from the reactor, respectively, are practically equal to the effluent and influent concentrations of the reservoir. Moreover, the substrate concentration (C_R) in the exit stream from the reservoir is the same than that within the stirred reservoir.

The variation of the mole-number of cellobiose in the reservoir of volume V in the time interval dt is:

$$-\mathrm{d}\,n = -V\mathrm{d}\,C_R = (C_R - C_F)\cdot u\ \mathrm{d}t \quad (4)$$

Taking into account the Equations 2 and 3, it can be obtained:

$$-\mathrm{d}C_R = C_R \cdot \left(1-\exp(-k\theta)\right)\cdot \frac{u}{V}\mathrm{d}\,t \quad (5)$$

$$-\frac{\mathrm{d}C_R}{C_R} = \frac{1-\exp(-k\theta)}{k\theta}\frac{kv}{V}\mathrm{d}\,t \quad (6)$$

If k and θ values are sufficiently low, being the reaction rate low and the flow rate high, as above supposed, it can be considered that:

$$1-\exp(-k\theta) \approx k\theta \quad (7)$$

Then, Equation 6 can be rewritten as:

$$-\frac{\mathrm{d}C_R}{C_R} = \frac{kv}{V}\mathrm{d}\,t \quad (8)$$

and

$$-\frac{\mathrm{d}C_R}{\mathrm{d}t} = k_{obs}\,C_R \quad (9)$$

where:

$$k_{obs} = \frac{kv}{V} \quad (10)$$

A linear dependence of ln C_R *vs.* t can be obtained by integrating Equation 9:

$$\ln C_R = \ln C_R^{\circ} - k_{obs} \cdot t \quad (11)$$

Once k_{obs} has been obtained, the rate coefficent (k) can be easily computed by Equation 10.

It can be easily evaluated that the approximation deriving by Equation 7 causes an error ≤ 5% for a ratio $k/SV \leq 0.1$, being $SV = 1/\theta$ the *space velocity* [33].

3. Results and discussion

3.1. Catalyst characteristics

NBP is known to be an acid solid with high ratio of BAS to LAS, higher than, for example, niobium oxide. As NBP has to be used in cellobiose hydrolysis, a reaction requiring protonic acid sites, we wanted to increase the protonicity of its surface by hydrolyzing the Nb-O-P, Nb=O, P=O bonds with HCl solutions, aimed at increasing the surface acid hydroxyl concentration with positive consequences on the catalyst activity. Therefore, three other samples have been prepared from NBP, studied, and tested in the reaction of cellobiose conversion.

The amorphous property of NBP is well known and reported in the literature [38, 39]. Only after high thermal treatment (1100°C), a well crystallized sample is formed (β form of $NbOPO_4$). The studied NBP sample and those obtained by acidic treatment of NBP had all amorphous

character (Fig. S1 – Supporting Data). The elemental composition of the modified NBP samples did not differ significantly from that of the parent NBP (Table S1). A decrease of the Nb and P concentrations in the HCl treated samples in comparison with the parent NBP has been observed and it could suggest some leaching caused by the HCl treatment (Table S1).

The values of surface area of the NBP samples, measured by nitrogen adsorption and thermally treated at 120°C before the analysis, are listed in Table 1. The acidic treatment of NBP did not result in remarkable morphologic modifications of the obtained samples. The values of surface area of all the samples are comprised in the 105-115 $m^2 g^{-1}$ interval and those of pore volume between 0.28-0.30 $cm^3 g^{-1}$, except NBP10 that has little higher surface and pore volume, likely due to some decrease of particle size following the strong acid treatment (10 M in HCl). These results indicated that NBP is a resistant material able to sustain severe chemical treatments without any significant structural and morphologic modifications.

3.2. Intrinsic and Effective Surface Acid Properties

Our main effort has been directed towards the study of the acidic properties of NBP and related samples, which has been performed with different methods and under different conditions.

The total surface acid sites of the samples have been titrated with a basic probe (PEA) dissolved in two solvents: cyclohexane and water, to determine the *intrinsic* and *effective* acidity, respectively [18]. The comparison between the results of the titrations carried out in the two different basic solutions permitted us to demonstrate and quantify the already known *water-tolerant* properties of the acid sites of NBP. Moreover, more sound correlations between the catalyst activity and *effective* catalyst acidity (measured in water) can be obtained.

In order to fully understand the solid acidity, the study of the nature of the acid sites is another important subject that has been developed. The NBP and related samples studied possess both BAS and LAS at their surfaces; it is known that the catalytic activity and selectivity in any given reaction is affected by the nature, strength, and distribution of the different acid sites on the surface.

Spectrophotometric experiments of base adsorption and desorption at increasing temperatures can be made in order to control the BAS and LAS presence and their relative amount and acid strength. In this case, the experiments of base adsorption-desorption have been also carried out in the presence of water.

3.2.1 Acidity measurements by PEA-titrations in liquid

The intrinsic acidity of NBP measured in cyclohexane, which has been chosen for its apolar and aprotic characteristics, is very high both in terms of amount of total acid sites and of acid site strength. From the I run adsorption of PEA (Fig. 2, right side), the total amount of acid sites (PEA_{tot} in meq g^{-1}) could be determined by applying the Langmuir equation (Equation 1) to the adsorption data. The total amount of the titrated sites (Table 1) is in perfect agreement with our previous measurements [10]. The total amount of the acid sites for the other samples prepared from NBP (NBP01, NBP1, and NBP10) does not differ so much from that of NBP (Table 1), only a slight increase of the titrated sites has been observed. The acidity ranking, written in terms of PEA_{tot}, follows the sequence: NBP < NBP0.1 < NBP1 < NBP10. It appears that the acid treatments of NBP have led to samples with only a modest increase of acidity. The II run adsorptions of PEA in cyclohexane (Fig. 2, left side) were very low on all the samples. In this case, the amount of acid sites determined from the adsorption data by Equation 1 corresponded only to the weak acid sites (PEA_{weak}, in meq g^{-1}). The values of PEA_{weak} corresponded to the amount of PEA desorbed following the pure cyclohexane elution (see Experimental, 1.2. section). As a consequence, the acid strength of sites was very high for all samples. The strong acid sites (PEA_{strong}, in meq g^{-1}) corresponded, on average, to 87% of all sites titrated. Fig. 2 shows for all the samples the measured adsorption isotherms of PEA in cyclohexane; the I run adsorptions, in particular, have a well Langmuirian shape, typical of chemisorption, in agreement with the high acid strength of the sites.

A different *scenario* has emerged when the measurements of surface acidity were made in water (Table 1), these measurements correspond to *effective* acidity of the samples. It is known that

water (polar compound, with solvating ability, as well) reacts with Brønsted sites and decreases the acid site strength by solvating effects and H-bond formation. In addition, water can coordinate to Lewis sites, so avoiding them the possibility to perform their acid function [40, 41]. Therefore, when a solid acid is concerned, its acidity is expected to decrease in water, as already observed on several catalyst samples [10, 17, 18]. This is due to the solvation ability of water and to its other peculiar properties that allow the creation of strong interactions with the acid centers of the solid. Water has to be displaced by the basic probe in order to be adsorbed, and this is only possible if a strong acid-base bond is formed. It is also possible that water and the probe can find allocation in the coordination sphere of the acid center, as it has been demonstrated for Nb-centers in several catalyst samples [13].

The results reported in Table 1 indicate that in water only a slight decrease of the amount of the total acid sites was observed in comparison with the titrations made in cyclohexane (NBP maintained in water around 87% of its intrinsic acid sites while NBP0.1, NBP1, and NBP10 maintained in water around 75% of their intrinsic acid sites). The light decrease of acidity observed for all the samples confirmed the *water-tolerant* characteristics of the Nb-acid sites of niobium phosphate samples.

In water, the acid strength of the titrated sites was very much lower than that measured in cyclohexane. For NBP, only 31% of the effective acid sites are strong sites, while only 15%, on average, for NBP0.1, NBP1, and NBP10. As a general trend, the surface acid strength of the samples in water was lowered in comparison with that intrinsically possessed by the samples.

Fig. 3 shows the I and II isotherm runs of PEA adsorption in water for all the samples. A comparison between Fig.s 2 and 3 clearly shows the decrease of acid strength of the *effective* sites on all the sample.

The only slight differences of the results of intrinsic and effective acidities of NBP and related samples demonstrated that NBP is a very robust catalyst that does not suffer too much the hydrolytic effect of acidic solutions.

An interesting comparison of acidity can be done between NBP and the niobic acid sample, as emerged from Ref. 10. NBP has twice the number of total acid sites possessed by niobic acid in terms of intrinsic acidity (measured in cyclohexane) with a greater percentage of strong acid sites. Comparing the acidity of the two samples in water (effective acidity), NBP manifests almost double the total acid sites compared to niobic acid, while the strong acid sites of the two samples are very similar.

3.2.2 Nature of acid sites studied by FT-IR spectroscopy

Spectroscopic characterization works on niobium phosphate catalyst have confirmed the presence of both terminal P-OH and Nb-OH groups, the former leading to a slightly stronger Brønsted acidity than Nb-OH sites. Lewis acidity is also present on the surface and it has been associated with coordinatively unsaturated Nb(V) sites [14, 42], as recently was revealed by acetonitrile adsorption followed by FT-IR spectroscopy [43].

In this work, the spectroscopic experiments of pyridine adsorption-desorption on the NBP samples have been carried out in both the vapor and aqueous phases with the final aim of better understanding the reaction and deactivation mechanisms where these samples are involved. In Fig.s 4 and 5, the FT-IR desorption spectra at 150°C in the range of 1400-1700 cm^{-1} of pyridine contacted both in vapor phase and aqueous solution on NBP, NBP01, NBP1 and NBP10 catalysts are shown.

All the spectra exhibited the same bands pattern typical of Brønsted and Lewis-type surface acid sites, but showing different intensities. In particular, the sharp bands corresponding to the interaction of pyridine molecules with the LAS at 1448 cm^{-1} (ν_{19b} mode) and 1610 cm^{-1} (ν_{8a} mode) can be clearly observed, while the broad bands at 1540 cm^{-1} (ν_{19b} mode) and 1637 cm^{-1} (ν_{8a} mode) are assigned to BAS [35]. The quantitative determination of Lewis and Brønsted acid sites was made on the basis of bands located at 1448 cm^{-1} and 1540 cm^{-1} according to the procedure reported by Emeis [36]. The attribution of the band at 1480 cm^{-1} is more difficult but it is likely related to the

simultaneous interaction of pyridine on coupled Brønsted and Lewis sites. Furthermore, all the catalysts showed a weak band at 3665 cm^{-1} (not shown) before outgassing, reasonably attributable to the –OH stretching mode of surface hydrogenphosphate species, that became sharper with outgassing until 250°C [9]. Conversely, the band relative to the –OH stretching mode of free Nb–OH at 3708 cm^{-1} was almost never observed even at high temperature, thus making the surface P–OH groups mostly responsible for the Brønsted acidity. On the other hand, low–coordinated Nb sites in tetrahedral coordination could be responsible for the Lewis acidity, as proposed for very similar *water–tolerant* acid materials such as niobic acid ($Nb_2O_5 \cdot nH_2O$) and H_3PO_4–treated niobic acid [13].

Pyridine in aqueous solution was purposely employed to investigate the acidic properties of the catalysts mimicking the real working conditions (i.e. in aqueous solutions). The evolution of the band relative to the scissoring mode of adsorbed water molecule at 1620 cm^{-1} was followed in order to confirm the co-adsorption of water and pyridine also during desorption experiments [9] (Fig.s S2 and S3). In detail, in the samples contacted with pyridine in aqueous solution this band resulted more intense at 150°C with respect to the dry samples, confirming the higher presence of water at this temperature.

In Table 2 are summarized the results of the determination of the acid sites for all catalysts using both the two ways of investigation. From data collected with pyridine in vapor phase on NBP, the concentration of Brønsted and Lewis acid sites was found 0.047 and 0.080 meq g^{-1}, respectively, in line with previous reports in the literature with comparable material pretreatment [44]. The HCl treatment of NBP resulted in an overall increase of acidity of the samples (NBP01, NBP1, and NBP10), in particular the LAS doubled and the BAS almost tripled, except for the NBP10 catalysts where doubled. Moreover, the LAS/BAS concentration ratio remained practically unchanged even after the treatment with HCl 10 M. The observed differences could be justified at the light of the modification of the Nb and P surface composition (Table S1).

In the presence of water only the LAS concentration of NBP slightly decreased, reaching 0.058 meq g^{-1}, while the BAS remained practically unchanged (0.045 meq g^{-1}). On the contrary, the catalysts treated with HCl showed a very different behavior. Lewis acid sites showed remarkable tolerance to water, suffering only a negligible decrease, while the Brønsted acid sites decreased deeply. Only for the NBP10 catalyst, the concentration of Lewis acid sites almost halved, but in any case, it was almost the double with respect to the parent NBP catalyst.

Noteworthy, the acidic treatment of NBP with HCl had also a certain effect on the BAS population, their concentration being higher (when analyzed in vapor phase) in comparison with the values of untreated NBP; these new BAS have low acid strength and only a limited amount (on average 40%) was detected in the presence of water (Table 2). The different impact of water on the LAS and BAS population can be rationalized considering that in presence of water the hydrogenphosphate groups responsible for the Brønsted-type acidity undergo partial re-hydration, thus decreasing in number, whereas the Nb sites responsible for the Lewis-type acidity, even though re-hydrated [45], can coordinate simultaneously both water and probe molecules. As mentioned previously, this peculiar ability of the Nb sites to coordinate probe molecules even in presence of water can be ascribed to residual positive charge on Nb sites in tetrahedral coordination, as demonstrated by FT-IR investigation with carbon monoxide as probe molecule on niobic acid [13].

3.3. Catalytic conversion of cellobiose in water

From our past activity on the hydrolysis of the disaccharides, A120, among the organic catalysts, and NBP, among the inorganic catalysts, have shown the most interesting performances towards the hydrolysis of cellobiose under mild conditions (80°C) [33]. In general, NBP showed higher activity than niobic acid in the hydrolysis of disaccharides (sucrose, maltose, and cellobiose). For example, the values of rate constants for the sucrose hydrolysis were 0.33 h^{-1} and 0.045 h^{-1} on NBP and niobic acid, respectively [33].

Cellobiose hydrolysis is a simple and clean reaction that leads selectively to glucose formation. On NBP, the possibility of increasing the reaction temperature can have interesting consequences. First, higher hydrolysis rates, and in second place, the activation of consecutive reactions from the formed glucose, thus allowing the formation of highly appealing final products, such as HMF.

With this aim, we have deepened the study of cellobiose conversion on the NBP acid catalysts, in comparison with A120, by working in the temperature interval of 110-130°C and 80-110°C, respectively. The results showed, as expected, that A120 has better catalytic activity than NBP; at temperature of 110°C, its coefficient rate is ca. ten times higher (Table 3). A120 has also appreciable activity at lower temperatures; at 80°C, the obtained rate coefficient (0.08 h^{-1}) is in agreement with that already reported for the same reaction [33]. Temperature had a positive action on the catalytic performances of the two catalysts. On A120 after 50 h of reaction, cellobiose conversion was 9%, 60%, and 87% at 80°C, 100°C, and 110°C, respectively and on NBP after 50 h of reaction, cellobiose conversion attained 24%, 46%, and 70% at 110°C, 120°C, and 130°C, respectively. The temperature dependence of the reaction of cellobiose conversion was evaluated by the classical Arrhenius approach to obtain the activation energy (Table 3). Similar values of the activation energy have been calculated for A120 and NBP. This differs from what had been obtained working with the disaccharide sucrose (substrate very easy to hydrolyze); in that case the value of E_a of A120 was about half that of NBP catalyst [33].

The product-distributions observed on A120 and NBP differed significantly. Fig.s 6 and 7 report the distribution trends of reactant and products (reported in terms of milliequivalents of monosaccharide) as a function of reaction time at 110°C on the two catalyst samples; similar trends have been observed for the other studied temperatures of reaction. On A120, the conversion of cellobiose to glucose was the only reaction observed, in fact only glucose and very little amount of soluble by-products (<5 meq L^{-1} only at 110°C) were formed up to almost total cellobiose conversion (Fig. 6). On NBP at 110°C, the decrease of cellobiose concentration was not only much

slower than on A120 but during the reaction course, other products accompanied the glucose formation: among them, fructose, HMF, and CP1 were clearly detected. Selectivity to glucose attained ca. 35%, while selectivity to fructose was not higher than 3%. This behavior indicated that the peculiar acidity of NBP (co-presence of lively BAS and LAS in water) was able to isomerize in some part glucose to fructose, and the latter was involved in other consecutive reactions. This behavior was also observed on NBP at reaction temperatures of 120°C and 130°C; fructose selectivity was not higher than 3.5-4% while glucose selectivity attained 38-42%. It is known that fructose is more reactive than glucose and it can be easily converted in HMF by cyclo-dehydration reaction [46, 47]. Also, similar evidences as those above discussed were recently reported by Zhang et al. [9] that demonstrated the role of Lewis acids in aqueous solution in the isomerization of glucose to fructose, with further fructose dehydration to HMF. On NBP, the observed HMF was formed with selectivity of 15%, 26%, and 31% at 110°C, 120°C, and 130°C, respectively. Besides HMF, which constitutes a final stable product of cellobiose conversion, the formation of a heavier soluble condensation product (CP1) was observed, likely an oligomer of HMF, as our first analytical evidences seem to indicate. CP1 was evidenced in the HPLC chromatogram at the lowest retention time, typically the zone in which soluble oligosaccharides are observed. However, as CP1 was extracted from the aqueous solution containing the reaction products with methyl isobutyl ketone (MIBK), it should be associated to a compound different from oligosaccharides. CP1 was completely absent on A120, where any HMF was not formed, and it was observed on NBP with high yield (from 8% to 20% in the temperature interval 110-130°C after 50 h of reaction). Only at reaction temperature of 120° and 130°C, other soluble by-products were formed that summed up all together gave a total concentration around 5-7 meq L^{-1}.

The catalytic performances of NBP01, NBP1, and NBP10 were also tested in the temperature interval 110°-130°C. Cellobiose conversion and product distributions did not deeply differ from those observed on NBP, as the sample surfaces are not highly different from NBP. As a general trend, glucose was formed in high amount while low amount of fructose was always observed;

HMF and CP1 were the two final stable products. All the other by-products ranged from 4% to 10% of the total product formed in the temperature interval of the studied reaction (110°C-130°C). Fig. 8 shows for the four NBP samples the values of cellobiose conversion and yields to glucose, fructose, HMF, and CP1 obtained at 120°C after 24 h of reaction. Cellobiose conversions ranged from 30% to 40% and the yields of HMF were always similar to that of CP1; NBP01 displayed the most interesting results in terms of cellobiose conversion and yield to HMF.

The activity ranking of the NBP-samples has been calculated on the basis of the rate coefficients of the reaction of cellobiose conversion at 120°C: NBP01 > NBP10> NBP ≅ NBP1 (Table 4). The rate coefficient of NBP01 is almost double than that of NBP even though it has intrinsic and effective acidity similar to NBP. It can be considered that the effective acid strength of the sites of NBP01 is lower than that possessed by NBP and the LAS population is more important than that of NBP (Table 2). These differences should justify the highest activity of NBP01 among the other NBP-samples.

The E_a values for NBP, NBP01, and NBP10 are comprised in a short interval (115-126 kJ mol^{-1}), as well as the ln A values (35-38), as reported in Table 4. These low values of E_a have been obtained for the most active catalysts. Due to compensation effect often observed in the derivation of the activation parameters, respective ln A values are the low, too [48]. On the contrary, NBP1 has high E_a and ln A values associated with the lowest rate coefficient for the studied reaction of cellobiose conversion. This could be due to a non-balanced presence of LAS and BAS on its surface, which causes a lower reaction rate than the other NBP-catalysts. In the recent literature [9], the activity of niobium oxide and niobium phosphate catalysts used in the conversion of biomass-derived carbohydrates to HMF in water in relation with a balanced population of Lewis and Brønsted sites has been discussed.

It is known that the reaction of fructose to HMF, which has been observed on all the NBP-catalysts during cellobiose conversion, leads to catalyst deactivation for the formation of insoluble *humic materials* that precipitate on the catalyst surface, being highly insoluble in water [20, 49-51].

This phenomenon causes catalyst deactivation with consequences on lowering the rate of the main reaction, due to subtraction of part of active catalyst surface. The recent review of I. Sádaba et al. [52] discusses various phenomena responsible of catalyst deactivation in liquid media, in particular in reactions of biomass conversion, with attention to the possibility to reuse solid catalyst affected by deactivation.

On the NBP-catalysts, deactivation was guessed during the kinetic interpretation to the data to obtain the rate coefficients. As shown by Fig. 9, not perfectly linear trends (in particular, at the highest reaction temperature, 130°C) were obtained when plotting the linearized first order rate equation up to ca. 100 h of reaction. Focusing on the results obtained at 130°C, the computed values of the coefficient rates (k_{obs}) are 1.81 h^{-1} in the time interval 0-10 h and 0.94 h^{-1} in the time interval 20-30 h. The decreasing trend of the k_{obs} values with reaction time suggests deactivation of part of the catalyst surface.

An evaluation of the formation of insoluble products during the reaction was possible comparing the total chromatographic areas obtained analyzing the samples collected at the different reaction times with the initial area of cellobiose. The insoluble products, expressed in terms of mono-saccharides equivalents, were <5% of the fed cellobiose for the total reaction time (99 h) at 110°C, and up to 70 h and 30 h at 120 and 130°C, respectively. The insoluble products attained roughly 9-10% to 50 h at 130°C.

In order to study the catalyst deactivation, all the used NBP catalysts (after drying at 80°C) have been analyzed by thermogravimetric analysis (TGA) to investigate adsorbed surface organic species. Following the method described by Sahoo et al. [53], the thermogravimetric profiles can be divided in three-sub-intervals of temperature relevant to volatile organic compounds (VOCs, 50-180°C), soft-coke (180-330°C), and hard coke (330-800°C). Fig. 10 shows the TGA profiles and relative first derivative curves (DTGA) as a function of temperature for NBP after reaction at 110°C, 120°, and 130°C, taken as example. VOCs are present in the highest amount on NBP (DTGA peak at 170°C with a shoulder at 150°C) at any temperature, while hard-coke (DTGA peak

at 450°C) was only present on the catalyst after reaction at 120°C and, in particular, at 130°C. This signifies that the insoluble organic species formed during fructose dehydration reaction can convert and grow on the catalyst surface as a function of the reaction temperature, giving rise to coke. The formed coke could be removed by simple oxidative thermal treatments, allowing the reuse of the catalyst. The same experimental TGA evidences have been observed on all the other NBP-catalysts.

4. Conclusions

In summary, the good *water-tolerant* acid properties of niobium phosphate have been confirmed by base-titrations in water in comparison with those made in cyclohexane. In addition, the prevalent Lewis acidity of niobium phosphate catalysts in water has been proved by spectrophotometric evidences.

The key to successfully realizing the conversion of carbohydrate biomass to HMF is the balanced presence on the catalyst surface of both Brønsted and Lewis acid sites with lively acidity in the chosen reaction solvent. The cooperative action of the BAS and LAS can combine the first hydrolysis step with the isomerization and dehydration steps in a one-pot reaction system. The *effective* acidity of the NBP-samples is high and the *effective* acid strength can be suitable for activate substratse in given reactions.

The catalytic synthesis of HMF directly from polysaccharides can take advantage of catalysts possessing both Lewis and Brønsted acid sites on the surface, like NBP, with possibility to hydrolyze the polysaccharide by Brønsted acid sites, isomerize the monomer sugars formed by Lewis acid sites, and then dehydrate them to the final HMF product. To increase the HMF yield, the optimization of the acid catalyst with balanced LAS and BAS populations and the selection of a suitable solvent mixture with water would be the two actions to perform.

Acknowledgments

All the authors gratefully thank Dr. Matteo Marzo from Dipartimento di Chimica of Università degli Studi di Milano, Italy, for the experimental support.

Supporting Data

Scheme S1. Scheme of the cellobiose reaction to HMF.

Fig. S1: XRD patterns of NBP and one derived sample obtained from its acidic treatment.

Table S1: Element Analysis of NBP1 and NBP10 Evaluated by EDX.

Fig. S2: FT-IR desorption spectra in the region from 1550 cm^{-1} to 1710 cm^{-1} of NBP01 from room temperature to 250 °C with pyridine adsorbed in vapor phase.

Fig. S3: FT-IR desorption spectra in the region from 1550 cm^{-1} to 1710 cm^{-1} of NBP01 from room temperature to 250 °C with pyridine adsorbed in aqueous solution.

Supplementary data associated with this article can be found, in the online version, at the address: http://dx.doi.org/10.1016/j.apcatb.xxxxxxxxxx.

REFERENCES

(1) M. Ziolek, Catal. Today 78 (2003) 47-64.

(2) K. Tanabe, Catal. Today 78 (2003) 65-77.

(3) I. Nowak, M. Ziolek, Chem. Rev. 99 (1999) 3603-3624.

(4) T. Okuhara, Chem. Rev. 102 (2002) 3641-3666.

(5) S. Okazaki, M. Kurimata, T. Iizuka, K. Tanabe, Bull. Chem. Soc. Jpn. 60 (1987) 37-41.

(6) S.Okazaki, N. Wada, Catal. Today 16 (1993) 349-359.

(7) A. Florentino, P. Cartraud, P. Magnoux, M. Guisnet, Appl. Catal. A: Gen. 89 (1992) 143-153.

(8) Y. Zhang, J. Wang, J. Ren, X. Liu, X. Li, Y. Xia, G. Lu, Y. Wang, Catal. Sci. Technol. 2 (2012) 2485-2491.

(9) Y. Zhang, J. Wang, X. Li, X. Liu, Y. Xia, B. Hu, G. Lu, Y. Wang, Fuel, 139 (2015) 301-307.

(10) P. Carniti, A. Gervasini, S. Biella, A. Auroux, Chem. Mater. 17 (2005) 6128-6136.

(11) P.Carniti, A. Gervasini, S. Biella, A. Auroux, Catal. Today 118 (2006) 373-378.

(12) D. Ding, J. Wang, J. Xi, X. Liu, G. Lu, Y. Wang, Green Chem., 16 (2014) 3846-3853.

(13) K. Nakajima, Y. Baba, R. Noma, M. Kitano, J. N. Kondo, S. Hayashi, M. Hara, J. Am. Chem. Soc. 133 (2011) 4224–4227.

(14) T. Armaroli, G. Busca, C. Carlini, M. Giuttari, A.M. Raspolli Galletti, G. Sbrana, J. Mol. Catal. A: Chem. 151 (2000) 233-243.

(15) H. Shintaku, K. Nakajima, M. Kitano, N. Ichikuni, M. Hara, ACS Catal. 4 (2014) 1198-1204.

(16) K. Nakajima, R. Noma, M. Kitano, M.Hara, J. Phys. Chem. C, 117 (2013) 16028-16033.

(17) M.J. Campos Molina, M. López Granados, A. Gervasini, P. Carniti, Catal. Today 254 (2015) 90-98.

(18) P. Carniti, A. Gervasini, M. Marzo, Catal. Today 152 (2010) 42-47.

(19) I. van Zandvoort, Y. Wang, C.B. Rasrendra, E.R.H. van Eck, P.C.A. Bruijnincx, H.J. Heeres, B.M. Weckhuysen, ChemSusChem 6 (2013) 1745-1758.

(20) M. Marzo, A. Gervasini, P. Carniti, Catal. Today 192 (2012) 89-95.

(21) S. Van de Vyver, J. Geboers, A. Jacobs, B. Sels, ChemCatChem 3 (2011) 82-94.

(22) M.E. Himmel, S.Y. Ding, D.K. Johnson, W.S. Adney, M.R. Nimlos, J.W. Brady, T.D. Foust, Science 315 (2007) 804-807.

(23) S. Suganuma, K. Nakajima, M. Kitano, D. Yamaguchi, H. Kato, S. Hayashi, M. Hara, J. Am. Chem. Soc. 130 (2008) 12787-12793.

(24) Y. Roman-Leshkov, J.N. Chheda, J.A. Dumesic, Science 312 (2006) 1933-1937.

(25) P. Gallezot, Chem. Soc. Rev. 41 (2012) 1538-1558.

(26) X. Qi, M. Watanabe, T.M. Aida, R.L. Smith, Green Chem. 10 (2008) 799-805.

(27) S. Hu, Z. Zhang, J. Song, Y. Zhou, B.X. Han, Green Chem. 11 (2009) 1746-1749.

(28) C. Chatterjee, F. Pong, A. Sen, Green Chem. 17 (2015) 40-71.

(29) F.W. Lichtenthaler, Carbohydr. Res. 313 (1998) 69-89.

(30) T. Wang, M.W. Nolte, B.H. Shanks, Green Chem. 16 (2014) 548-572.

(31) M.J. Climent, A. Corma, S. Iborra, Green Chem. 16 (2014) 516-547.

(32) D.M. Alonso, S.G. Wettstein, M.A. Mellmer, E.I. Gurbuz, J.A. Dumesic, Energy Environ. Sci. 6 (2013) 76-80.

(33) M. Marzo, A. Gervasini, P. Carniti, Carbohydr. Res. 347 (2012) 23-31.

(34) P. Carniti, A. Gervasini, Biella, S. Adsorpt. Sci.Technol. 23 (2005) 739-749.

(35) M. Tamura, K. Shimizu, A. Satsuma, Appl. Catal. A: Gen. 433 (2012) 135–145.

(36) C. A. Emeis, J. Catal. 141 (1993) 347–354.

(37) S.K. Sahoo, S.S. Ray, I.D. Singh, Appl. Catal. A: Gen. 278 (2004) 83–91.

(38) Martins, R.L.; Schitine, W.J., Castro, F.R. Catal. Today 5 (1989) 483-491.

(39) M.H.C. de la Cruz, F.C. da Silva, E.R. Lachter, Catal. Today 118 (2006) 379-384.

(40) W.L. Jorgensen, J.M. Briggs, J. Am. Chem. Soc. 111 (1989) 4190–4197.

(41) J.C. Védrine, Res. Chem. Intermed. 41 (2015) 9387-9423.

(42) R. Turco, A. Aronne, P. Carniti, A. Gervasini, L. Minieri, P. Pernice, R. Tessera, R. Vitiello, M. Di Serio, Catal. Today 254 (2015) 99-103.

(43) H. Gomez Bernal, A.M. Raspolli Galletti, G. Garbarino, G. Busca, E. Finocchio, Appl. Catal. A: Gen. 502 (2015) 388-398.

(44) A. S. Rocha, A. M. S. Forrester, M. H. C. de la Cruz, C. T. da Silva, E. R. Lachter, Catal. Commun. 9 (2008) 1959-1965.

(45) Q. Sun, Y. Fu, H. Yang, A. Auroux, J. Shen, J. Mol. Catal. A: Chem. 275 (2007) 183-193

(46) R. J. van Putten, J.C. van der Waal, E. de Jong, C. Rasrendra, H.J Heeres, J.G. de Vries, Chem. Rev. 113 (2013) 1499-1597.

(47) R. Lopes de Souza, H. Yu, F. Rataboul, N. Essayem, Challenges 3 (2012) 212-232.

(48) I. Plazl, S. Leskovšek, T. Koloini, Chem. Eng. J. 59 (1995) 253-257.

(49) S.K.R. Patil, C.R.F. Lund, Energy Fuels (2011) 25, 4745-4755.

(50) S.K.R. Patil, J. Heltzel, C.R.F. Lund, Energy Fuels 26 (2012) 5281-5293.

(51) I. van Zandvoort, Y. Wang, C.B. Rasrendra, E.R.H. van Eck, P.C.A. Bruijnincx, H.J. Heeres, B.M. Weckhuysen, ChemSusChem 6 (2013) 1745-1758.

(52) I. Sádaba, M. López Granados, A. Riisagerc, E. Taarning, Green Chem., 17 (2015) 4133-4145.

(53) S.K. Sahoo, S.S. Ray, I.D. Singh, Appl. Catal. A: Gen. 278 (2004) 83-91.

Tables and Figures

Table 1. Main Properties of the Catalyst Samples.

Table 2. Determination of the nature of the acid sites determined by FT-IR with pyridine (PY) as probe molecule in absence and in presence of water

Table 3. Rate coefficients and kinetic parameters for the reaction of conversion of cellobiose in water on the catalysts A120 and NBP

Table 4. Rate coefficients and kinetic parameters for the reaction of conversion of cellobiose in water on NBP and derived catalysts 120°C

Fig. 1. Scheme of the catalytic reaction line used for the catalytic tests of cellobiose conversion to HMF working in complete recirculation of the liquid aqueous solution; the catalytic reactor worked between 80° and 130°C under pressure.

Fig. 2. Isotherms at 30°C of PEA adsorption in cyclohexane (*intrinsic* acidity) on all the catalyst samples; I run adsorption (right) and II run adsorption (left).

Fig. 3. Isotherms at 30°C of PEA adsorption in water (*effective* acidity) on all the catalyst samples; I run adsorption (right) and II run adsorption (left).

Fig. 4. FT-IR desorption spectra at 150 °C of pyridine on NBP (a), NBP01 (b), NBP1 (c) and NBP10 (d), with pyridine adsorbed in vapor phase. Brønsted (BAS) and Lewis (LAS) acid sites peaks at 1540 and 1448 cm^{-1}, respectively.

Fig. 5. FT-IR desorption spectra at 150°C of pyridine on NBP (a), NBP01 (b), NBP1 (c) and NBP10 (d), with pyridine adsorbed in aqueous solution. Brønsted (BAS) and Lewis (LAS) acid sites peaks at 1540 and 1448 cm^{-1}, respectively. Scissoring mode band (W) of adsorbed water molecules at 1620 cm^{-1}.

Fig. 6. Distribution trends of CEL (□) and GLC (◊) in the reaction of conversion of cellobiose in water on A120 catalyst at 110°C (concentration in terms of mequivalent of monosaccharide).

Fig. 7. Distribution trends of CEL (□), GLC (◊), FRU (Δ), HMF (○), and CP1 (+) in the reaction of conversion of cellobiose in water on NBP catalyst at 110 °C (concentration in terms of mequivalent of monosaccharide).

Fig. 8. Comparative results of the reaction of conversion of cellobiose on NBP, NBP01, NBP1, and NBP10 catalysts: conversion and yield to the reaction products evaluated at 120°C after 24 h of reaction.

Fig. 9. Deactivation trend in the reaction of cellobiose transformation on NBP at 110°C (□), 120°C (Δ), and 130°C (○) as a function of reaction time. (cellobiose concentration in meq L^{-1}).

Fig. 10. TGA (red) and DTGA (black) profiles in air atmosphere as a function of temperature (10°C min^{-1}) of used NBP after reaction at 110°C (A), 120°C (B), and 130°C (C).

Table 1. Main Properties of the Catalyst Samples

Sample	Specific Surface Area [a] / $m^2\ g^{-1}$	Pore Volume a / $cm^3\ g^{-1}$	Total Acid Sites (**I.A.**) [b] PEA_{tot}/ meq g^{-1}	Strong Acid Sites (**I.A.**) [b] PEA_{strong}/ meq g^{-1}	Total Acid Sites (**E.A.**) [b] PEA_{tot}/ meq g^{-1}	Strong Acid Sites (**E.A.**) [b] PEA_{strong}/ meq g^{-1}
NBP	115	0.30	0.403	0.353 (88%) [c]	0.350	0.108 (31%) [c]
NBP01	105	0.29	0.437	0.378 (87%)	0.344	0.0430 (12%)
NBP1	110	0.28	0.439	0.379 (86%)	0.313	0.0496 (16%)
NBP10	144	0.35	0.450	0.395 (88%)	0.349	0.057 (16%)

[a] Thermal treatment of activation: 120°C for 2 h under vacuum (10^{-3} mbar).

[b] Adsorption temperature, 30°C; solvent, cyclohexane for *intrinsic* acidity (I.A.) and water for *effective* acidity (E.A.) measurements.

[c] Percent of strong acid sites.

Table 2. Determination of the nature of the acid sites determined by FT-IR with pyridine (PY) as probe molecule in absence and in presence of water

Sample	$Py_{(vap)}$ [a]			$Py_{(aq)}$ [b]		
	LAS /meq g^{-1}	BAS /meq g^{-1}	LAS/BAS	LAS /meq g^{-1}	BAS /meq g^{-1}	LAS/BAS
NBP	0.080	0.047	1.69	0.058	0.045	1.30
NBP01	0.151	0.123	1.23	0.121	0.029	4.25
NBP1	0.157	0.118	1.33	0.121	0.052	2.35
NBP10	0.159	0.093	1.72	0.095	0.040	2.40

[a] Pyridine contacted in vapor phase. [b] Pyridine contacted in aqueous solution.

Table 3. Rate coefficients and kinetic parameters for the reaction of conversion of cellobiose in water on the catalysts A120 and NBP

Sample	Temperature / °C	Rate coefficient [a] / h^{-1}	E_a / kJ mol^{-1}	ln A [b]
A120	80	0.08	119 ± 2	38 ± 1
	100	0.86		
	110	1.97		
NBP [c]	110	0.29	115 ± 6	35 ± 2
	120	0.76		
	130	1.81		

[a] k (see 2.4. paragraph for calculation); [b] A / h^{-1}; [c] evaluated in the first part of the reaction.

Table 4. Rate coefficients and kinetic parameters for the reaction of conversion of cellobiose in water on NBP and derived catalysts 120°C

Sample	Rate coefficient [a] / h^{-1}	E_a / kJ mol^{-1}	ln A [b]	Rate coefficient ratio k_{cat}/k_{NBP}
NBP	0.76	115 ± 6	35 ± 2	-
NBP01	1.44	125 ± 32	38 ± 10	1.90
NBP1	0.70	166 ± 3	50 ± 1	0.92
NBP10	1.08	126 ± 10	38 ± 3	1.42

[a] *k* (see 1.3.2.paragraph for calculation), evaluated in the first part of the reaction; [b] A / h^{-1}.

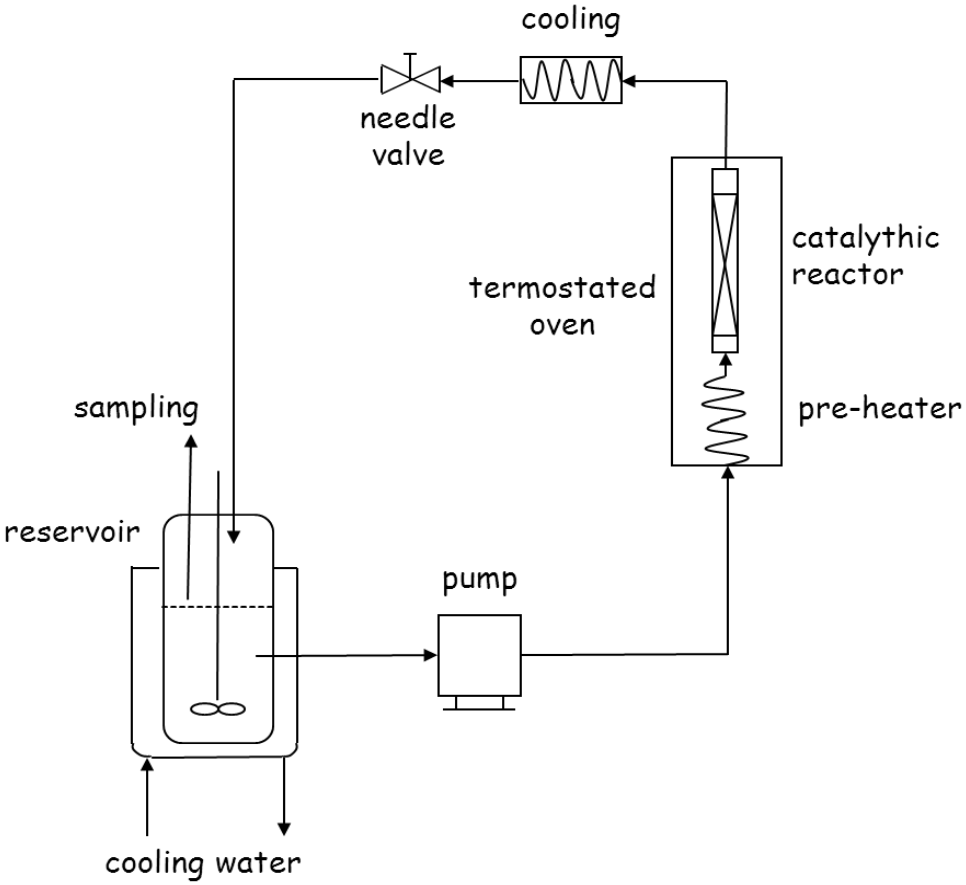

Fig. 1. Scheme of the catalytic reaction line used for the catalytic tests of cellobiose conversion in complete recirculation of the aqueous solution; the catalytic reactor worked between 80° and 130°C under pressure.

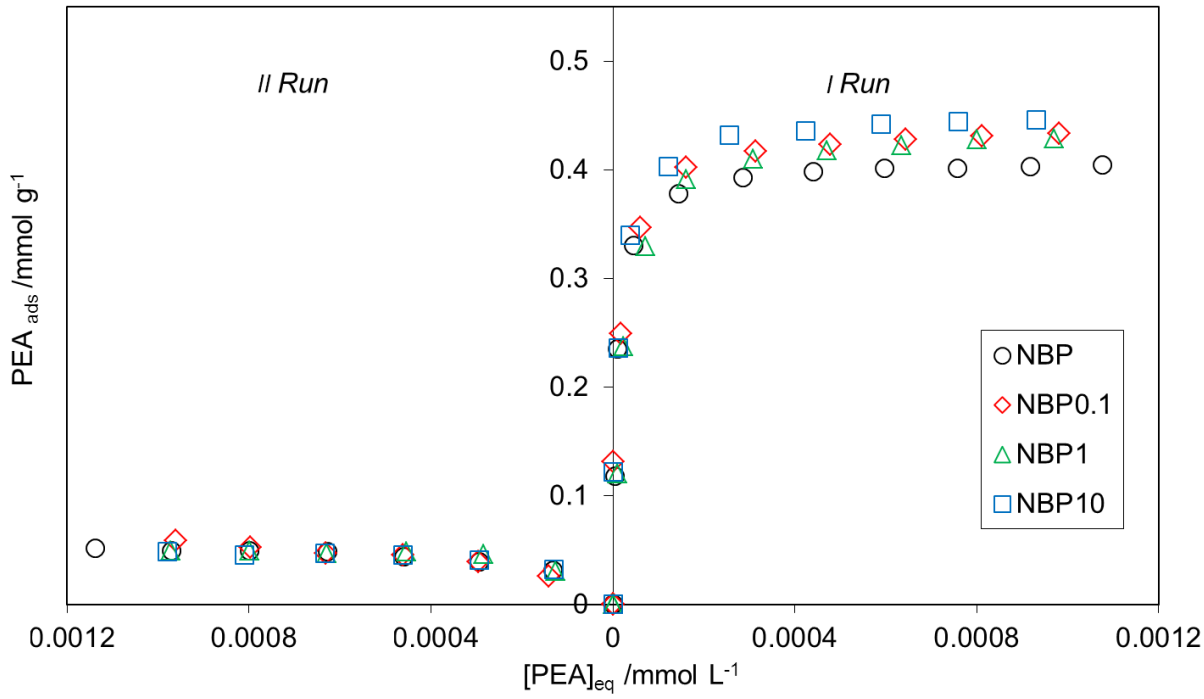

Fig. 2. Isotherms at 30°C of PEA adsorption in cyclohexane (*intrinsic* acidity) on all the catalyst samples; I run adsorption (right) and II run adsorption (left).

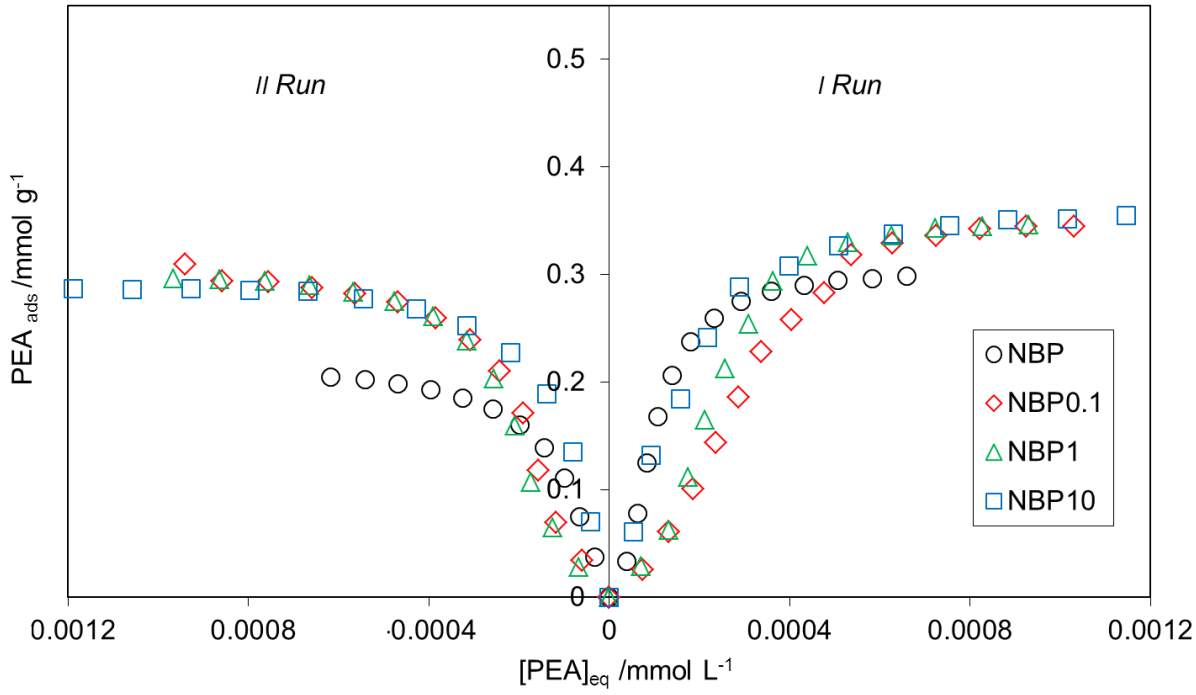

Fig. 3. Isotherms at 30°C of PEA adsorption in water (*effective* acidity) on all the catalyst samples; I run adsorption (right) and II run adsorption (left).

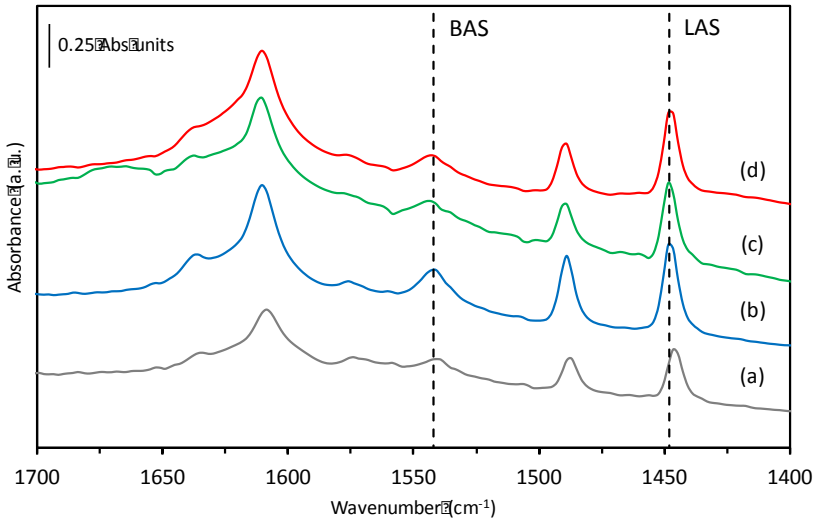

Fig. 4. FT-IR desorption spectra at 150 °C of pyridine on NBP (a), NBP01 (b), NBP1 (c) and NBP10 (d,) with pyridine adsorbed in vapor phase. Brønsted (BAS) and Lewis (LAS) acid sites peaks at 1540 and 1448 cm^{-1}, respectively.

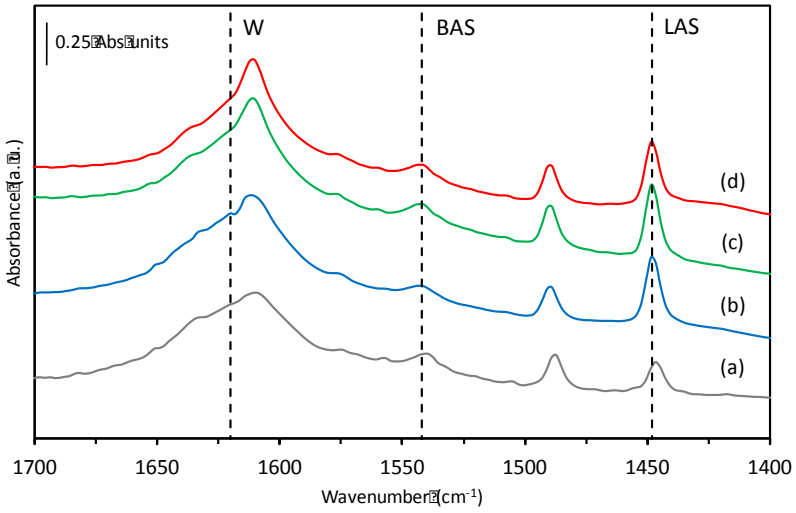

Fig. 5. FT-IR desorption spectra at 150 °C of pyridine on NBP (a), NBP01 (b), NBP1 (c) and NBP10 (d), with pyridine adsorbed in aqueous solution. Brønsted (BAS) and Lewis (LAS) acid sites peaks at 1540 and 1448 cm^{-1}, respectively. Scissoring mode band (W) of adsorbed water molecules at 1620 cm^{-1}.

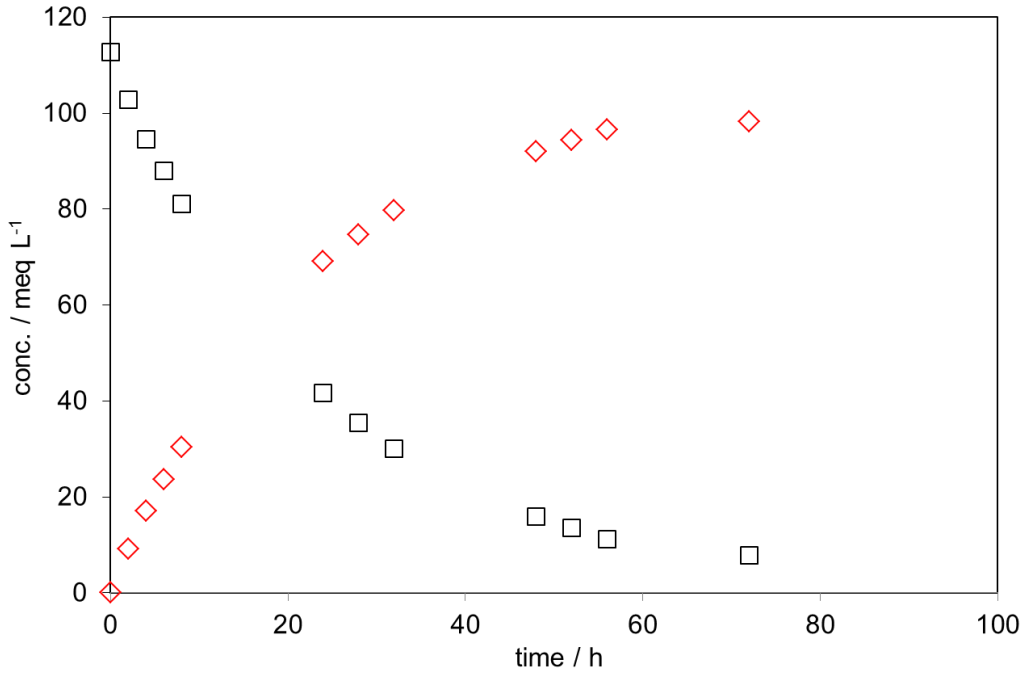

Fig. 6. Distribution trends of CEL (□) and GLC (◊) in the reaction of conversion of cellobiose in water on A120 catalyst at 110°C (concentration in terms of mequivalent of monosaccharide).

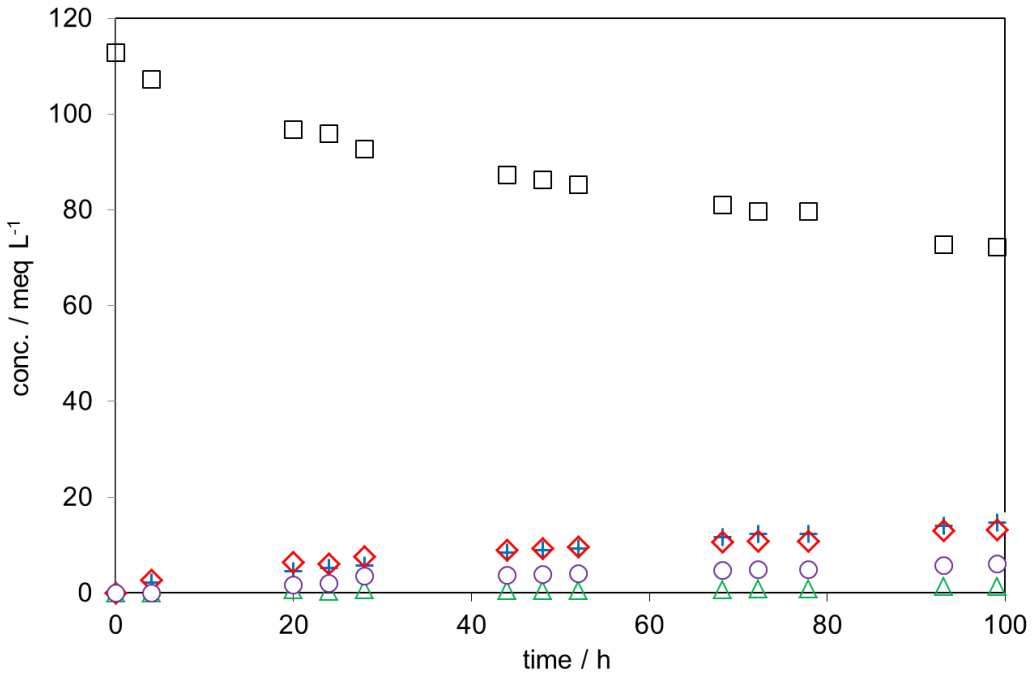

Fig. 7. Distribution trends of CEL (□), GLC (◊), FRU (Δ), HMF (○), and CP1 (+) in the reaction of conversion of cellobiose in water on NBP catalyst at 110 °C (concentration in terms of mequivalent of monosaccharide).

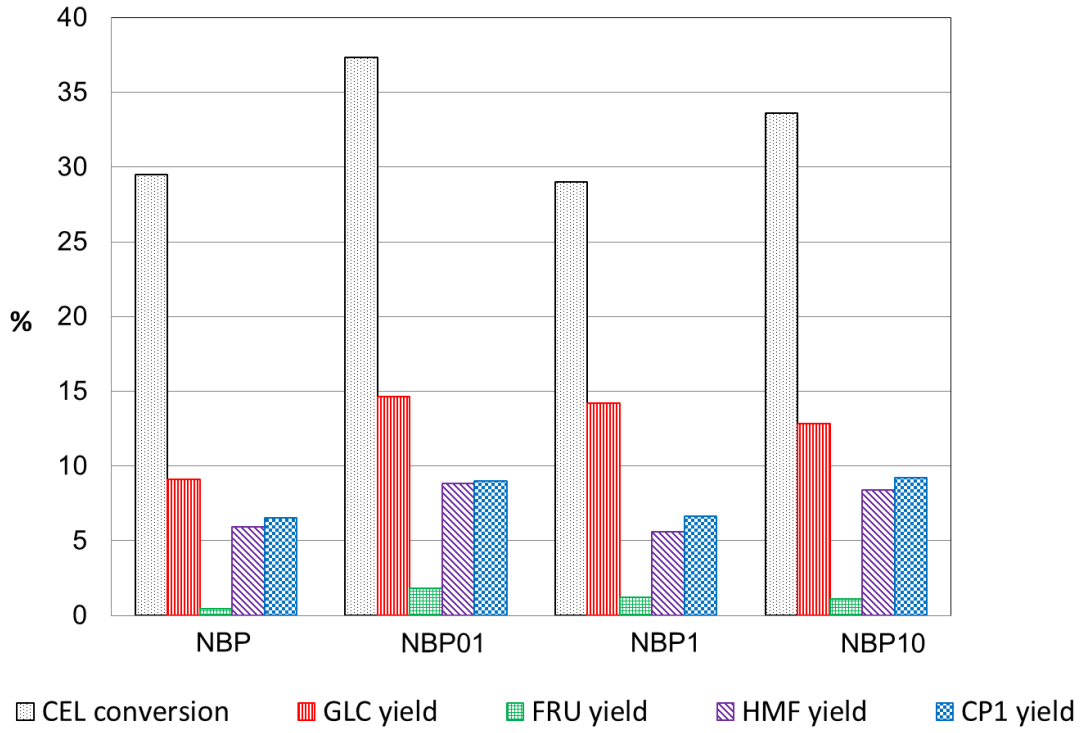

Fig. 8. Comparative results of the reaction of conversion of cellobiose on NBP, NBP01, NBP1, and NBP10 catalysts: conversion and yield to the reaction products evaluated at 120°C after 24 h of reaction.

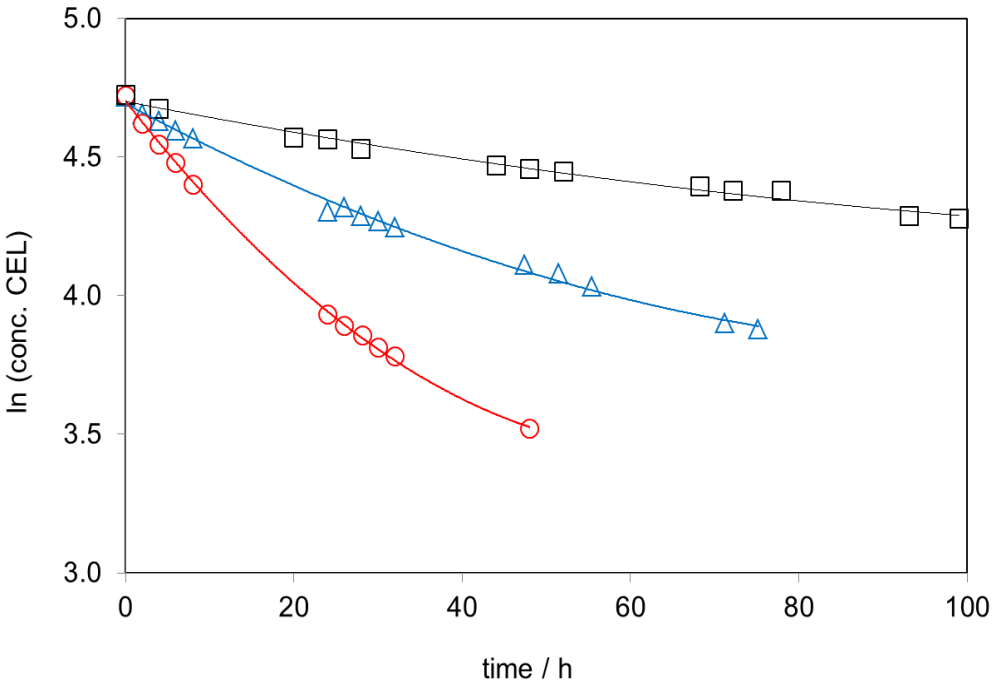

Fig. 9. Deactivation trend in the reaction of cellobiose transformation on NBP at 110°C (□), 120°C (Δ), and 130°C (○) as a function of reaction time. (cellobiose concentration in meq L^{-1}).

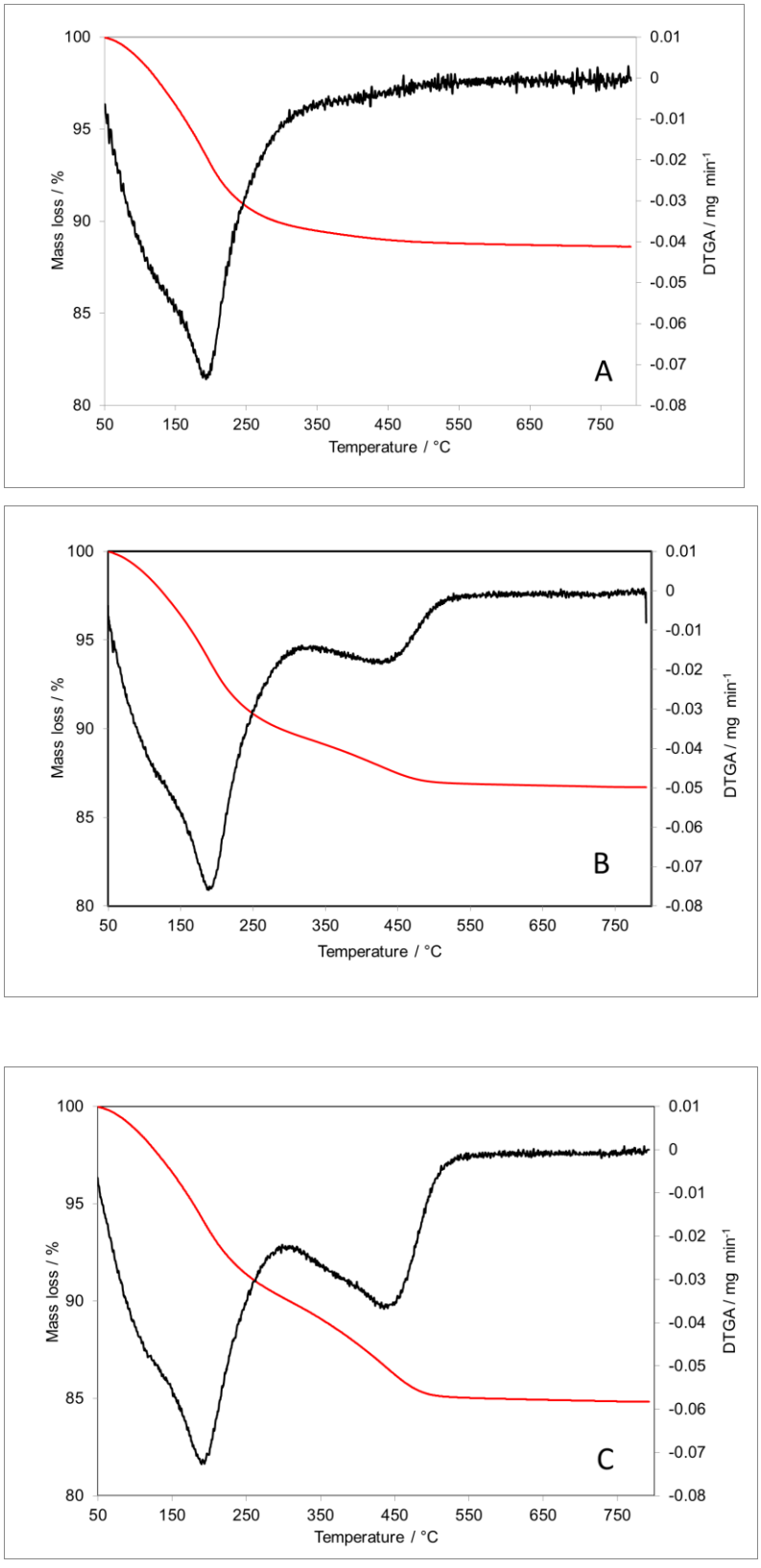

Fig. 10. TGA (red) and DTGA (black) profiles in air atmosphere as a function of temperature (10°C min^{-1}) of used NBP after reaction at 110°C (A), 120°C (B), and 130°C (C).

*Graphical Abstract

Graphical Abstract

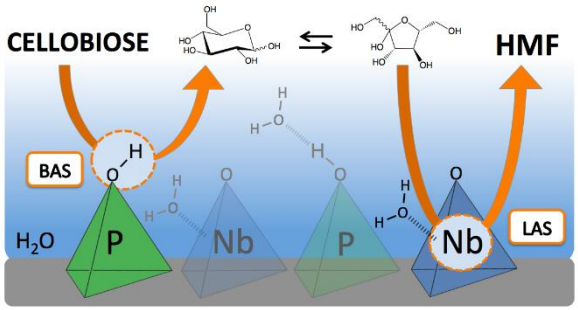

Highlights

- Niobium phosphate catalyst and modified samples by acidic treatments were used in water.
- Direct reaction of cellobiose to hydroxymethylfurfural (HMF) was studied in water.
- Comparative results with a sulfonic acid resin (Amberlite IR120) were obtained.
- The *effective* acidity of the catalysts was measured in different solvents.
- The acid site nature in water was studied by FT-IR spectra byan adsorbed basic probe

Supplementary Material

Click here to download Supplementary Material: SUPPORTING Data.docx